fractal and fractional

MDPI

Article

The Influence of Fly Ash Dosages on the Permeability, Pore Structure and Fractal Features of Face Slab Concrete

Lei Wang [1,2,*], Shihua Zhou [3,*], Yan Shi [3], Yajun Huang [1], Feng Zhao [1], Tingting Huo [1] and Shengwen Tang [4]

[1] School of Intelligent Construction, Wuchang University of Technology, Wuhan 430002, China
[2] College of Materials Science and Engineering, Xi'an University of Architecture and Technology, Xi'an 710055, China
[3] Changjiang River Scientific Research Institute, Wuhan 430072, China
[4] State Key Laboratory of Water Resources and Hydropower Engineering Science, Wuhan University, Wuhan 430072, China
* Correspondence: wanglei535250684@xauat.edu.cn (L.W.); zhoush@mail.crsri.cn (S.Z.)

Abstract: Concrete-face slabs are the primary anti-permeability structures of the concrete-face rockfill dam (CFRD), and the resistance of face slab concrete to permeability is the key factor affecting the operation and safety of CFRDs. Herein, the influences of five fly ash dosages (namely 10%, 20%, 30%, 40% and 50%) on the permeability property of face slab concretes were investigated. Moreover, the difference in the permeability caused by the fly ash dosage variations is revealed in terms of the pore structure and fractal theory. The results illustrate that: (1) The inclusion of 10–50% fly ash lowered the compressive strength of face slab concretes before 28 days of hydration, whereas it contributed to the 180-day strength increment. (2) The incorporation of 10–50% fly ash raised the average water-seepage height (D_m) and the relative permeability coefficient (K_r) of the face slab concrete by about 14–81% and 30–226% at 28 days, respectively. At 180 days, the addition of fly ash improved the 180-day impermeability by less than 30%. (3) The permeability of face slab concretes is closely correlated with their pore structures and D_s. (4) The optimal fly ash dosage in terms of the long-term impermeability and pore refinement of face slab concretes is around 30%. Nevertheless, face slab concretes containing a high dosage of fly ash must be cured for a relatively long period before they can withstand high water pressure.

Keywords: face slab concrete; permeability; pore; air void; fractal dimension

Citation: Wang, L.; Zhou, S.; Shi, Y.; Huang, Y.; Zhao, F.; Huo, T.; Tang, S. The Influence of Fly Ash Dosages on the Permeability, Pore Structure and Fractal Features of Face Slab Concrete. *Fractal Fract.* **2022**, *6*, 476. https://doi.org/10.3390/fractalfract6090476

Academic Editor: Zine El Abiddine Fellah

Received: 5 August 2022
Accepted: 25 August 2022
Published: 28 August 2022

1. Introduction

The concrete-face rockfill dam (CFRD) is a common dam type throughout the world. CFRD comprises of a rockfill as the main body of the dam, and the concrete-face slabs as the primary anti-permeability structure [1–3]. CFRDs are constructed all over the world due to their superior seismic performance, high adaptability to geological and climate conditions, low cost and short construction period [2,4,5]. Concrete-face slabs are thin structures with a large surface area to thickness ratio. In the last three decades, CFRDs have been rapidly developed in China, including the Gongbaxia CFRD (132 m) in Qinghai province, the Aertashi CFRD (164.8 m) and Dashixia CFRD (247 m) in Xinjiang province, etc. Generally, CFRDs are often designed to have a dam height level of 100 m to 300 m, which means the water pressure caused by the high water head is immense. Therefore, the face slab concretes used in these projects are required to have a good permeability resistance to water penetration. Considering that concrete-face slabs are the primary anti-permeability structures of CFRDs, their impermeability is one of the key factors affecting the operation and safety of CFRDs [6,7].

Fly ash is a by-product of coal combustion in thermal power plants. Its major components are quartz, mullite and some glassy phases, which can react with $Ca(OH)_2$ [8–11]. Fly ash is widely used in CFRDs, in practice, to improve the workability and cracking

resistance of face slab concrete. Generally, adding a suitable amount of fly ash to concrete has a positive effect on the impermeability of the concrete. Abu et al. [12] found that fly ash addition at a level below 15% reduced the chloride penetration in fiber concrete by about 69% at 90 days, while increasing the content of fly ash increased the chloride penetration by up to 30% at 90 days. Bog and Topçu [13] also reported that, when the fly ash dosage exceeded 15%, the chloride penetration in the concrete increased. Liu et al. [14] and Kizilkanat et al. [15] pointed out that, when the fly ash dosage was greater than 30%, the charge passed into the concrete at 28 days began to increase. In addition, many studies confirmed that, before 28 or 90 days of hydration, concrete containing 30–50% fly ash showed weaker impermeability than the plain concrete [16], whereas at a long-term age (i.e., 180 days), it exhibited a comparable chloride penetration or water permeability coefficient [12,17].

The permeability resistance of concrete depends on the pore structures of the concrete [18,19]. A numerical model proposed by Zheng et al. [20] showed that the permeability is governed by the porosity and microgeometry of the pore structures. Metha and Monterio [21] stipulated that the permeability of concrete is closely correlated with the pores, with sizes ranging between 0.05–0.1 μm. Wu et al. [22] obtained the similar results based on a series of transport property experiments and proposed that the water and chloride penetration of concrete is highly dependent on the fractions of pores with sizes ranging from 0.01 to 0.1 μm, rather than those with a size exceeding 0.1 μm. Nevertheless, there are no studies regarding the influence of the fly ash dosage on the impermeability and pore structures of face slab concrete.

To remedy the aforementioned issue, the effects of fly ash added in five dosages, including 10%, 20%, 30%, 40% and 50%, on the impermeability of face slab concrete were studied. In addition, the differences in the degree of impermeability caused by changing the fly ash dosage were interpreted in terms of the pore structures and fractals. Fractal geometry is an effective method for studying the complex and irregular features of pore structures [23–28], which provided a new point of view for understanding the influence of the fly ash dosage on the impermeability of face slab concretes in this study. The results may help engineers to select proper fly ash dosages in order to design concrete-face slab with a strong impermeability.

2. Materials and Analytical Methods

2.1. Raw Materials

Portland cement (CEM I with a 28-day compressive strength of 48.6 MPa), conforming to GB 175 [29], was used to prepare the concretes. An ASTM Type F Fly ash was utilized to partially replace the Portland cement in the concretes. The physical features and chemical compositions of cement and fly ash are exhibited in Table 1. Crushed limestone with a maximal size of 40 mm was utilized as the coarse aggregate, the specific gravity of which was 2.67. The fine aggregate was also crushed limestone with a fineness modulus of 2.80 and a specific gravity of 2.66. The saturated surface dry (SSD) condition was achieved before the aggregates were used to produce the concrete.

2.2. Mix Proportions

The mix proportions of the face slab concretes were experimentally determined according to Chinese specification DL/T 5016 (design code for concrete-faced rockfill dams) [30]. In practice, face slab concrete is commonly designed to have a moderate 28-day compressive strength, ranging between 35 and 45 MPa. In this study, six concrete mixtures containing 0%, 10%, 20%, 30%, 40% and 50% fly ash (by the weight of the cement) were designed. These mixtures were designated as C0, CFA10, CFA20, CFA30, CFA40 and CFA50, respectively. A water reducer and an air-entraining agent (AEA) were added to these mixtures to obtain a slump value of around 60 mm and an air content of around 5%. The mix proportions are presented in Table 2.

Table 1. Physical features and oxides of the cement and fly ash.

Oxides	Oxides (wt. %)	
	CEM I PC	Fly Ash
CaO	62.72	3.02
SiO_2	20.32	53.69
Fe_2O_3	4.46	10.87
Al_2O_3	4.42	24.96
MgO	3.92	2.85
SO_3	2.37	0.35
R_2O *	0.41	1.07
Ignition loss (%)	1.04	2.32
Physical features		
Specific gravity	3.22	2.33
Specific surface area by Blaine (m^2/kg)	332	395
Fineness (residue on a 45 μm sieve %)	8.4	6.5
Strength activity index	-	81

* Alkali content (R_2O) = Na_2O + 0.658K_2O.

Table 2. Mix proportion of the face slab concretes.

Notations	W/B Ratio	Fly Ash Dosage (%)	Mix Proportion (kg/m^3)							Air Content (mm)	Slump (mm)
			Water	Cement	Fly Ash	Sand	Coarse Aggregate	Water Reducer	AEA		
C0	0.38	0	124	326	0	617	1316	2.28	0.07	4.8	52
CFA10	0.38	10	124	294	33	613	1309	2.28	0.07	4.8	54
CFA20	0.38	20	124	261	65	610	1301	1.96	0.07	4.9	57
CFA30	0.38	30	124	228	98	607	1294	1.96	0.08	4.8	58
CFA40	0.38	40	124	196	131	603	1287	1.96	0.08	4.7	60
CFA50	0.38	50	124	163	163	600	1280	1.96	0.10	4.8	64

2.3. Test Method

2.3.1. Compressive Strengths of the Face Slab Concretes

Compressive strengths of the face slab concretes were determined, complying with DL/T 5150 [31]. Three hydration ages were selected as 3, 28 and 180 days, which referred to the early hydration time, middle hydration time and long-term hydration time, respectively. The fresh concrete was molded into 150 mm × 150 mm × 150 mm steel molds. After being demolded, they were cured in a high-moisture room (20 ± 2 °C and RH larger than 95%). Six samples were tested, and the average value was adopted as the final compressive strength.

2.3.2. Impermeability

Face slab concretes are required to possess a good degree of impermeability to prevent water penetration caused by high water pressures. The impermeability test was conducted through the water-seepage height determination, complying with the standard DL/T 5150, adopting a permeability instrument with the Hp-4.0 model. The permeability of the concrete at 28 and 180 days was tested in this study, while the permeability test at 3 days was not conducted, since the face slab concrete could not bear the water pressure load used in practice at this early age.

For each permeability test, six cylindrical samples with a top diameter of 185 mm, a bottom diameter of 150 mm and a height of 175 mm were tested for each mixture proportion. Prior to the tests, the circular surface of the sample was covered with a layer of hot wax. After that, the samples were placed in the machine and tested. During the test, the water pressure was kept constant at 1.2 MPa for 24 h. Then, the experiment was ceased, and each cylindrical sample was split into two parts. The average value of the water-seepage height (D_m) for each sample was measured based on the determination at 10 points. The relative

permeability coefficient (K_r) of the concrete can be determined by Equation (1) [31], which is shown below:

$$Kr = aD_m^2/2TH \quad (1)$$

where K_r is the relative permeability coefficient, cm/h; T is the duration of the permeability test, which was 24 h in this study; H is the water head (cm) corresponding to a constant water pressure of 1.2 MPa, which, herein, was 12,244 cm; and a is the absorption ratio of the concrete, which was at a constant value of 0.03.

2.3.3. Pore Structure Analysis Using a Mercury Intrusion Porosimeter (MIP)

In this work, the porosity and pore size distribution of the face slab concretes cured for 3, 28 and 180 days were measured by MIP, using a mercury intrusion porosimeter (AutoPore IV 9500 type, manufactured by Micromeritics Instruments Corporation, Norcross, GA, USA). The mercury intrusion pressure range is 0–414 Mpa, which is suitable for probing pores sized from approximately 2 nm to 10 µm. The small samples with a size about 5 mm used for the MIP tests were cut from the inner part of the concrete specimens. Prior to the MIP tests, the coarse aggregates were extracted from the small samples to avoid the large aggregate effects. Four small samples were added to the sample tubes for each MIP test, minimizing the influence of sample size variations on the test results.

2.3.4. Calculation Method of the Fractal Dimension

The pores in concrete, which are complex and inhomogeneous, are regarded as the key factor influencing the permeability of concrete [32–35]. Recent studies confirmed that the fractal geometry can characterize and explain the roughness and irregularities of the pores in concrete to a considerable extent. The fractal dimensions of concrete have been proven to be closely correlated with the concrete's macro-performance [24,36]. There are many kinds of fractal models that can be used to calculate the fractal dimensions, among which Zhang's fractal model [37,38], based on MIP results, is the most frequently used. In this work, Zhang's fractal model was adopted to determine the fractal dimensions of the pore surfaces (D_s) of the face slab concrete. According to Zhang's theory, the accumulated injection work on mercury (W_n) is logarithmically correlated with the total injected mercury volume (V_n) during the MIP test, and the relationship between them can be revealed by Equation (2):

$$ln\frac{W_n}{r_n^2} = D_s ln\frac{V_n^{1/3}}{r_n} + C \quad (2)$$

where r_n refers to the pore radius, m (meter); n refers to the n-th mercury injection; and C represents the regression constant.

W_n can be calculated by Equation (3):

$$W_n = \sum_i^n p_i \triangle V_i \quad (3)$$

where the index I denotes the i-th mercury injection, which is between 1 and n; p_i refers to the mercury pressure, Pa; and V_i is the injected volume of the mercury at the i-th injection, m (meter)^3.

The W_n, V_n, $ln\frac{W_n}{r_n^2}$ and $ln\frac{V_n^{1/3}}{r_n}$ values can be determined using the MIP results and Equation (3). Subsequently, the D_s can be calculated by Equation (2), since D_s is the slope of the straight line in Equation (2). In addition, the determination coefficient (R^2) of the fitting line was also calculated in order to evaluate the accuracy and reliability of the D_s.

3. Results and Discussion

3.1. Compressive Strength of the Face Slab Concrete

The compressive strengths of the face slab concretes containing different dosages of fly ash at 3, 28 and 180 days are shown in Figure 1. Figure 1 also shows the errors in the compressive strength results.

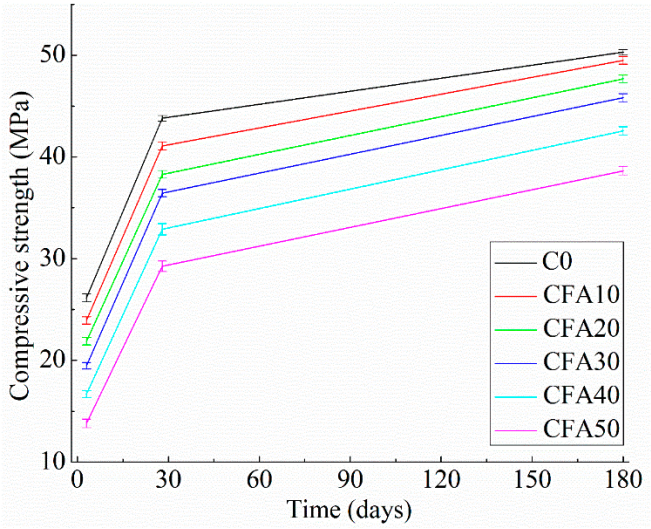

Figure 1. Compressive strength results of the face slab concretes cured at 3, 28 and 180 days.

Figure 1 shows the compressive strength of the face slab concretes with an enhanced hydration age. Figure 1 also indicates that the fly ash addition had a strong influence on the development of the compressive strength of the face slab concretes.

After 3 days, the compressive strengths of the face slab concretes had declined by 8.5%, 16.4%, 25.6%, 36.2% and 47.2% due to the inclusion of 10%, 20%, 30%, 40% and 50% fly ash, respectively, compared with that of the C0 concrete. These reductions can be explained by the inert features of the fly ash at 3 days, when fly ash cannot participate in the pozzolanic reaction [39]. As a quantitative study revealed, the degree of the fly ash's reaction in concrete is about 3% at 3 days [40]. As expected, the replacement of the cement with fly ash decreased the amount of cement and, therefore, the concrete's strength.

After 28 days, the reductions in the compressive strength were about 6.2%, 12.6%, 16.8%, 24.9% and 33.2%, respectively, compared with the C0 concrete, due to the inclusion of 10%, 20%, 30%, 40% and 50% fly ash. It was observed that the discrepancy between the strengths of the fly ash concrete and C0 concrete became smaller compared to that at 3 days, indicating that the fly ash addition may contribute to the development of the strength at 28 days. As many studies indicated [40–44], the 28-day reaction degree of fly ash is 9–23%, which means that the fly ash begins to participate in the pozzolanic reaction at 28 days.

However, as the hydration process extended to 180 days, the discrepancy in compressive strength between the fly ash concretes and C0 concrete became much smaller. For instance, the CFA10 concrete and CFA20 concrete exhibited almost the same compressive strength as the C0 one at 180 days, and the 180-day compressive strengths of the CFA30, CFA40 and CFA 50 concretes were about 8.9%, 15.4% and 23.2% lower than that of the C0 one, respectively. These findings demonstrate that the fly ash became highly involved into the pozzolanic reaction at 180 days, which aided the increment in the strength of the concrete at this long hydration age. A similar long-term compressive strength increase in fly ash concrete was reported by other studies [41,42]. In general, the long-term increase in the compressive strength can be attributed to the pozzolanic reaction of the fly ash with $Ca(OH)_2$ [43]. The quantitative study proved that the reaction degree of the fly ash in concrete is about 26%–33% at 180 days [40,44]. This pozzolanic reaction can produce a large number of C–S–H, improving the micro-structure and the long-term strength of the concrete [45–48].

3.2. Water Permeability of the Face Slab Concrete

The permeability test results at 28 and 180 days, including the average water-seepage height (D_m) and the relative permeability coefficient (K_r), are presented in Table 3. From

Table 3, it can be seen that the fly ash dosage had a significant influence on the impermeability of the face slab concretes.

Table 3. The permeability results of the face slab concretes with fly ash at 28 and 180 days.

Designations	Hydration Time (Days)	Average Water-Seepage Height D_m (cm)	Relative Permeability Coefficient K_r ($\times 10^{-7}$ cm/h)
C0	28	3.6 ± 0.19	6.62 ± 0.70
	180	2.8± 0.12	4.00 ± 0.34
CFA10	28	4.1 ± 0.15	8.58 ± 0.63
	180	2.5 ± 0.14	3.19 ± 0.36
CFA20	28	4.6 ± 0.14	10.8± 0.66
	180	2.3 ± 0.11	2.70 ± 0.26
CFA30	28	5.2 ± 0.15	13.8 ± 0.79
	180	1.9 ± 0.13	1.84 ± 0.25
CFA40	28	5.6 ± 0.16	16.0 ± 0.92
	180	2.1 ± 0.12	2.25 ± 0.26
CFA50	28	6.5 ± 0.17	21.6 ± 1.13
	180	3.7 ± 0.13	6.99 ± 0.49

Table 3 shows that the addition of 10–50% fly ash was detrimental to the impermeability of the face slab concrete at 28 days, and a higher dosage of fly ash was accompanied by a weaker impermeability. Specifically, the addition of 10% fly ash increased the D_m and K_r values of the C0 concrete by about 14% and 30%, respectively. When the fly ash dosage was raised to 50%, the CFA50 exhibited 28-day D_m and K_r values of 6.5 cm and 21.6 $\times$ 10^{-7} cm/h, respectively, which were approximately 81% and 226% greater than those of the C0 concrete. This weakened impermeability resulting from the addition of fly ash before 28 days was also reported by Liu et al. [14] and Kizilkanat et al. [15]. This experimental phenomenon is caused by the weak reactivity of the fly ash at the early and middle age, as well as its dilution effects. As demonstrated by other studies [40,44,46,49], the fly ash begins to react at 28 days and cannot contribute greatly to the improvement of the microstructure of the concrete. At the same time, the inclusion of fly ash reduces the amount of cement in the concrete mixture and, as a consequence, decreases the amount of hydration products which could can the pore structure and improve the impermeability of the concrete.

In addition, at 180 days, it can be observed from Table 3 that the fly ash addition, at a dosage of less than 30%, clearly improved the 180-day impermeability of the face slab concrete compared with that of the C0 concrete. Specifically, the inclusion of 10% fly ash lowered the D_m and K_r of the C0 concrete by approximately 11% and 20% at 180 days, respectively. When the substitution rate of the fly ash reached 30%, the CFA30 concrete exhibited D_m and K_r values about 32% and 54% lower, respectively, as compared to those of the C0 one at 180 days.

Nevertheless, Table 3 shows that, beyond the fly ash dosage of 30%, the fly ash addition negatively affected the 180-day impermeability of the face slab concrete. For instance, with the fly ash dosage was raised from 30% to 40%, the D_m and K_r values slightly increased from about 1.9 cm and 1.84 $\times$ 10^{-7} cm/h to about 2.1 cm and 2.25 $\times$ 10^{-7} cm/h, respectively. The further increase in the fly ash dosage to 50% significantly raised the D_m and K_r values to about 3.7 cm and 6.99 $\times$ 10^{-7} cm/h, which were about 32% and 75% greater than those of the C0 concrete, respectively. These results correspond well with findings reported by another study [16], which revealed that concretes containing 30–50% fly ash have a weaker impermeability than plain concrete. As stated by Moghaddam et al. [50], a proper dosage of fly ash can cause the cementitious matrix of the concrete to become dense through the filler effect and the ball-bearing effect resulting from the spherical shape of the fly ash particles, leading to an improved impermeability. Moreover, the pozzolanic reaction of the fly ash with $Ca(OH)_2$ at the late hydration age can produce C–S–H gels, which are able to fill the pore structures and densify the microstructures, cutting off the water and ion penetration

channels in the concretes [22]. However, beyond a dosage of 30%, the fly ash addition may be detrimental to the concrete's impermeability.

The above results indicate that the optimal fly ash dosage, in terms of the long-term impermeability of face slab concrete, is considered to be around 30%. Additionally, face slab concrete containing a high dosage of fly ash must be cured for a relatively long period before it can withstand a high level of water pressure. It is widely reported that the permeability property is closely related with the pore structures of concretes. Zheng et al. [20] proved that the permeability is governed by the porosity and micro-geometry of the porous structures of concretes. In this work, the improved impermeability may be also due to the modification of the pore structures of the face slab concrete. This point of view is discussed and verified in terms of the pore structures in the following section.

3.3. Pore Structures of the Face Slab Concrete

The porosity, the pore size distribution and the most probable pore size of the face slab concretes containing 0–50% dosages of fly ash and cured for 3, 28 and 180 days are exhibited in Table 4. According to the classical method developed by Mindess et al. [51] for classifying pores, the pores of a size between 2.5 nm to 10 nm can be categorized as small capillary (or gel) pores, pores between 10 nm to 50 nm are medium capillary pores, and pores between 50 nm and 10 μm are large capillary pores. From Table 4, we can see that the pore structures of all the concrete specimens in this study became more refined and denser as the hydration process continued.

Table 4. Pore structure parameters of the face slab concretes containing different dosages of fly ash.

Notation	Hydration Age (Day)	The Most Probable Pore Size (nm)	Porosity (%)	Pore Size Proportions		
				<10 nm (%)	10–50 nm (%)	50 nm–10 μm (%)
C0	3	169	27.6	8.1	31.2	60.3
	28	65	20.5	14.5	46.9	37.8
	180	42	18.4	18.5	50.2	30.9
CFA10	3	181	29.2	7.5	28.3	63.7
	28	72	22.4	13.6	44.8	41.5
	180	37	17.1	20.6	50.7	28.6
CFA20	3	191	31.4	6.9	26.1	66.3
	28	78	23.5	13.2	42.9	43.8
	180	32	16.2	23.1	53.1	23.5
CFA30	3	206	33.1	5.8	24.2	69.3
	28	91	25.9	12.5	40.3	45.6
	180	25	14.8	24.8	54.6	20.3
CFA40	3	214	35.3	4.9	22.3	72.7
	28	100	27.2	10.9	39.1	49.6
	180	26	15.9	22.7	51.3	25.6
CFA50	3	221	39.6	3.1	18.4	78.3
	28	145	31.5	8.7	36.2	54.9
	180	60	21.3	19.3	48.9	31.3

Additionally, from Table 4, we can see that the fly ash dosage had a significant effect on the pore structures of the concretes. At 3 and 28 days, as the fly ash dosage was raised from 0% to 50%, the pores in the concrete became larger and coarser. For instance, the CFA10 concrete exhibited a 3-day porosity of 29.2%, a 3-day most probable pore size of 181 nm and proportion of large capillary pores (50 nm–10 μm) of 63.7%, which were about 1.6%, 12 nm and 3.4% greater than those of the C0 concrete, respectively, demonstrating that the inclusion of fly ash coarsened the pores in the concretes at 3 days. When the fly ash dosage reached 50%, a 3-day porosity, most probable pore size and proportion of large capillary pores of 39.6%, 221 nm and 78.3% were observed for the CFA50 concrete, which were 12%, 52 nm and 18% greater than those of the C0 one, respectively. The same trend can be observed for the face slab concretes containing fly ash cured at 28 days. These trends

are also due to the dilution effects and the weak reactivity of the fly ash at an early and middle hydration age [23–25].

It can be seen from Table 4 that, at 180 days, with a fly ash dosage of 30%, the fly ash markedly refined the pore structures of the face slab concretes, and a higher dosage of fly ash seemed to have a better refinement effect. Specifically, the 180-day porosity, the most probable pore size and the proportion of large capillary pores of the CFA10 concrete were reduced by 1.3%, 5 nm and 2.3% compared with those of the C0 one. This refinement effect became more obvious as the fly ash dosage increased to 30%. The CFA30 concrete exhibited a 180-day porosity, most probable pore size, and a proportion of large capillary pores of 14.8%, 25 nm and 20.3%, which were about 3.6%, 17 nm and 10.6% less than those of the C0 concrete, respectively. This pore refinement effect is due to the pozzolanic reaction between the fly ash and $Ca(OH)_2$ at a long-term age, producing a large quantity of C–S–H to fill up the pores in the concrete and leading to the refined pore structures [45,46].

Nevertheless, this refinement effect weakened or disappeared when the fly ash dosage exceeded a critical dosage of 30%. From Table 4, it is clear that the inclusion of 40% fly ash slightly coarsened the pore structures of the concrete compared with the inclusion of 30% fly ash at 180 days. At a fly ash dosage of 50%, remarkably coarsened pore structures, i.e., a greatly increased 180-day porosity, most probable pore size, and proportion of large capillary pores were observed for the CFA50 concrete compared with the CFA30 one and C0 one. The coarsened pore structures caused by the high fly ash beyond the dosage of 30% is likely due to the fact that the amount of $Ca(OH)_2$ was nearly completely consumed by the fly ash when the fly ash dosage exceeded 30%. According to the quantitative studies on the $Ca(OH)_2$ content in cement pastes cured for 180 days [49], the $Ca(OH)_2$ amount was about 17% in neat cement pastes, whereas it was about 6% in pastes containing 30% fly ash, and it was nearly negligible for cement pastes containing 40–60% fly ash. Therefore, an optimal fly ash dosage of 30%, in terms of the pore refinement effect, can be obtained.

3.4. Pore Surface Fractal Dimensions (D_s) of the Face Slab Concretes

Table 5 exhibits the D_s values of the face slab concretes containing fly ash at different dosages. On the basis of fractal theories, the D_s values of a porous object are within the range of 2.0–3.0. A D_s value close to 3.0 implies that the porous object has an extremely rough and complex pore structure. On the contrary, as the D_s approaches 2.0, the pore structure becomes smoother and turns into a smooth plane [23,52].

Table 5. D_s of the face slab concretes containing fly ash at different dosages.

Notations	Hydration Age (Day)	D_s	R^2
C0	3	2.836	0.963
	28	2.887	0.945
	180	2.911	0.989
CFA10	3	2.823	0.963
	28	2.872	0.986
	180	2.925	0.975
CFA20	3	2.816	0.963
	28	2.861	0.979
	180	2.934	0.967
CFA30	3	2.788	0.958
	28	2.852	0.963
	180	2.947	0.979
CFA40	3	2.763	0.963
	28	2.839	0.959
	180	2.941	0.977
CFA50	3	2.743	0.969
	28	2.819	0.958
	180	2.885	0.981

Table 5 indicates that the D_s values of all of the face slab concretes in this study ranged between 2.743 and 2.947, with very high determination coefficients (R^2) ranging between 0.945 and 0.989. The high R^2 values demonstrate the accuracy and reliability of the D_s. Based on the fractal theories, it can be concluded that the pore structure of the face slab concretes with a 0–50% dosage of fly ash in this study exhibited obvious fractal features.

The relationship between the pore structure parameters and D_s is shown in Figure 2. The volume proportions of the fine pores (with a pore size below 50 nm), which are abbreviated as $V_{2.5–50\ nm}$ thereafter and presented in Table 6, are determined by adding the proportions of the medium capillary pores and gel pores. From Figure 2, we can see that the parameters such as the porosity, the most probable pore size and $V_{2.5–50\ nm}$ are strongly correlated with the D_s, exhibiting determination coefficients (R^2) of 0.986, 0.903 and 0.951, respectively. This close relationship illustrates that the D_s could be used to precisely evaluate and characterize these pore structure parameters. Similar findings were obtained by other researchers [23,36,52]. As Jin et al. [36] pointed out, in contrast to the existing pore structural parameters, such as porosity and pore size, the index D_s can be used to evaluate the pore structures of concretes more precisely and comprehensively.

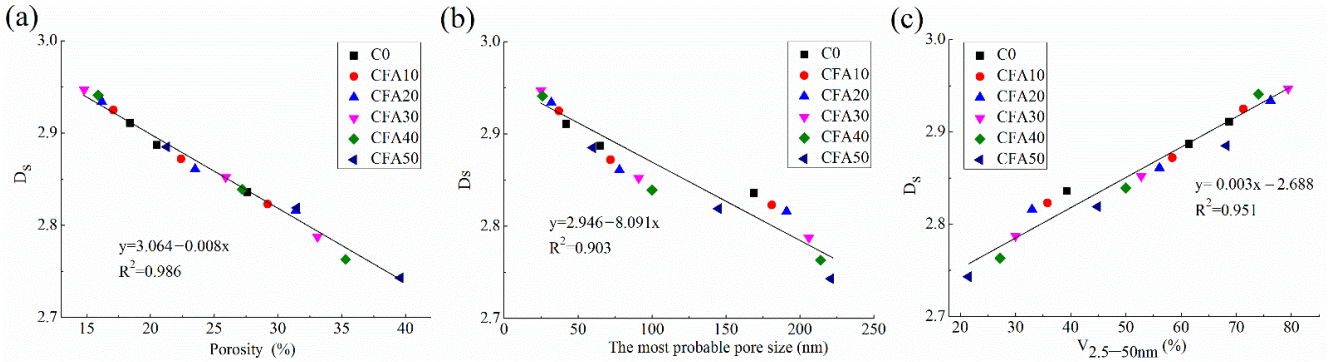

Figure 2. Relationship between D_s and (**a**) porosity, (**b**) the most probable pore size and (**c**) $V_{2.5–50\ nm}$.

Table 6. $V_{2.5–50\ nm}$ of the face slab concretes containing fly ash at different dosages.

Notations	Hydration Age (Days)	$V_{2.5–50\ nm}$ (%)
C0	3	39.3
	28	61.4
	180	68.7
CFA10	3	35.8
	28	58.4
	180	71.3
CFA20	3	33.0
	28	56.1
	180	76.2
CFA30	3	30.0
	28	52.8
	180	79.4
CFA40	3	27.2
	28	50.0
	180	74.0
CFA50	3	21.5
	28	44.9
	180	68.2

Moreover, to better understand the influences of the fly ash dosage on the D_s, the relationship between the D_s and the fly ash dosages is revealed and illustrated in Figure 3.

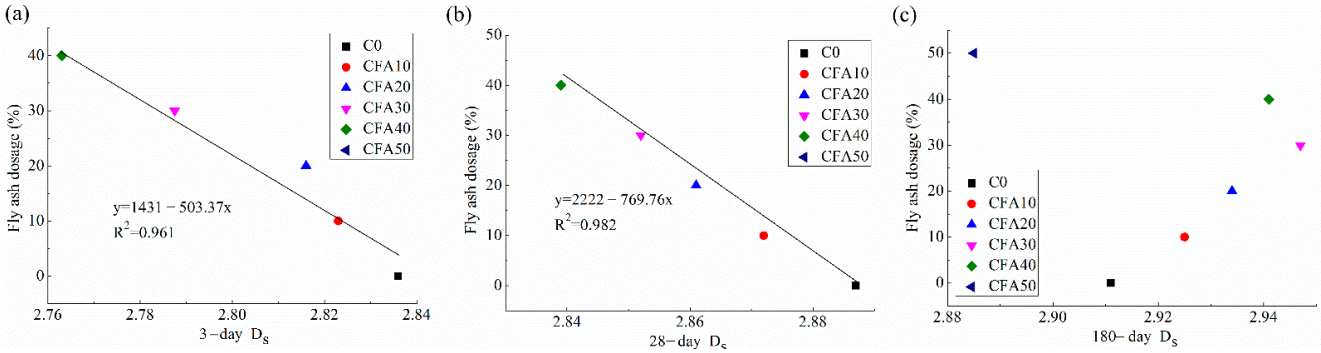

Figure 3. The relationship between the fly ash dosages and (**a**) 3-day D_s, (**b**) 28-day D_s and (**c**) 180-day D_s.

Figure 3 clearly shows that, at 3 and 28 days, the D_s values were reduced due to the fly ash inclusion. As the fly ash dosage was raised from 0 to 50%, the D_s values declined from 2.836 to 2.743 at 3 days, and from 2.887 to 2.819 at 28 days. This is because the inclusion of fly ash at an early and middle age coarsened the pore structure and produced a large number of large capillary pores, as revealed by the MIP results above.

Figure 3 also indicates that, at 180 days, the inclusion fly ash under the dosage of 30% increased the D_s values of the face slab concretes. For instance, when the fly ash dosage increased from 0 to 30%, the D_s values at 180 days were raised from 2.911 to 2.947. This is because the increase of the fly ash dosage to 30% made the pore structure finer and more complex. In fact, refined pores and enlarged D_s values were observed for concretes added with mineral admixtures, such as silica fume [25,53] and granulated blast furnace slag [23]. Generally, the pozzolanic reaction between such mineral admixtures and $Ca(OH)_2$ effectively densifies the pore structures and enhances the complexity and irregularity of the pores, leading to an increase in the D_s values of concretes, mortars or cement pastes.

Nevertheless, when the fly ash content was increased from 30% to 50%, the D_s values ceased increasing and reduced slightly from 2.947 to 2.885 at 180 days. As for the case of the 50% dosage, the D_s value of the CFA50 concrete was even lower than that of the C0 concrete. This experimental finding can be explained as follows: a fly ash dosage as high as 50% coarsened the pore structure; i.e., it reduced the $V_{2.5–50\,nm}$ values and increased the proportion of large capillary pores, thus reducing the complexity and irregularity of the pores and resulting in relatively low D_s values.

3.5. Pore Structural and Fractal Analysis of the Fly Ash's Influence on the Permeability

3.5.1. Pore Structural Analysis of the Permeability

The water permeability of the face slab concrete was investigated in terms of the pore structures and the correlations between pore structure parameters, such as the porosity and proportion of large capillary pores, and the relative permeability coefficients (K_r) at 28 and 180 days were plotted. They are exhibited in Figure 4.

Figure 4 illustrates that there were strong correlations between the K_r and pore structure parameters. Specifically, the K_r increased with the porosity as well as the proportion of large capillary pores. The same result was reported by Zheng et al. [20], who proved that the total porosity significantly affects the permeability of concrete. Similarly, Metha and Monterio [21] revealed that large pores (0.05–0.1 μm) have a strong influence on the permeability. This is because a large porosity and a large proportion of large capillary pores are helpful for the formation of permeable channels and facilitate water penetration and ion transportation. Hence, the differences in the degree of permeability caused by the fly ash dosages can be interpreted in terms of the pore structures.

As revealed by the MIP results, at 28 days, when the fly ash content was raised from 0 to 50%, the pores in the concretes became larger and coarser, leading to a continuous increase in the K_r values. At 180 days, at a fly ash dosage of 30%, the fly ash participated in the pozzolanic reaction, refined the pores and cut off the permeable channels, thus

enhancing the permeability resistance of the concrete to water penetration. However, the increase of the fly ash dosage from 30% to 50 % considerably coarsened the pore structures of the concrete at 180 days, which in turn clearly enlarged the K_r values. Taking into account the fact that face slab concretes are subjected to high water pressures solely at an advanced hydration age, the fly ash dosage utilized for face slab concrete is suggested to be no larger than 30% in practice.

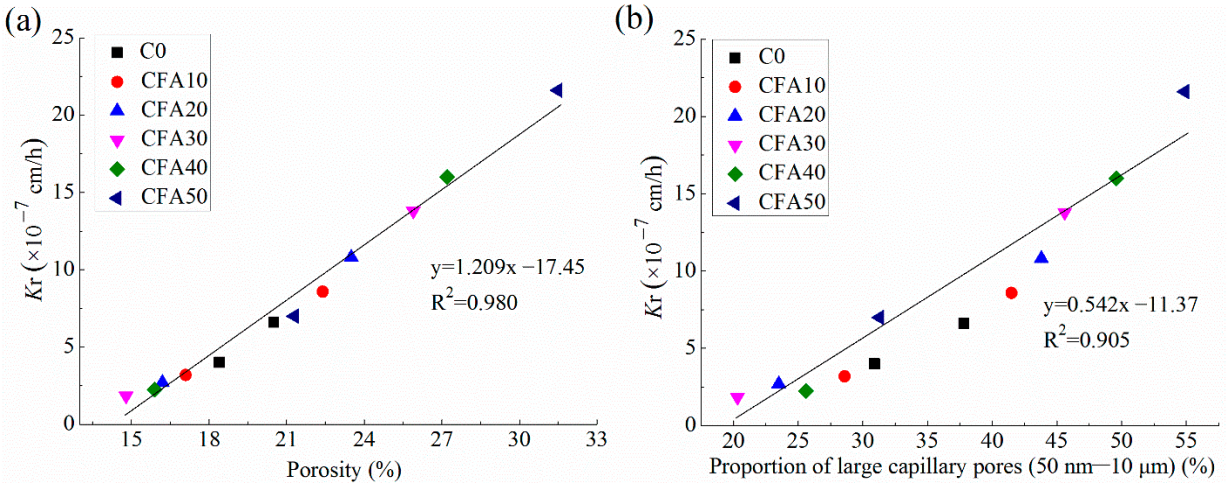

Figure 4. The relationship between the relative permeability coefficient K_r and (**a**) porosity and (**b**) proportion of large capillary pores.

3.5.2. Fractal Analysis of the Permeability

The water permeability of the face slab concrete was analyzed from the viewpoint of fractal theory, and the relationship between the K_r and D_s is shown in Figure 5.

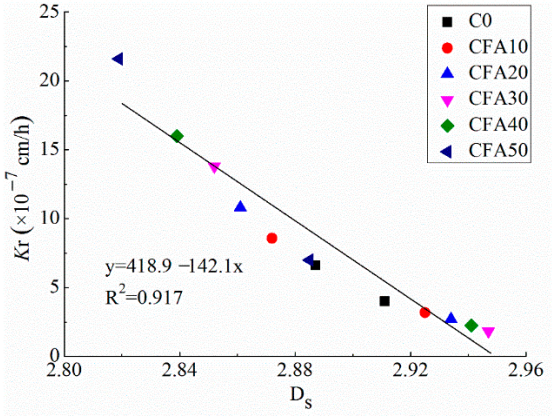

Figure 5. The relationship between K_r and D_s.

Figure 5 indicates that there was a negative relationship between the Kr and D_s, exhibiting an R^2 value of 0.917. That is to say, the high permeability (corresponding to the high K_r values) of the concrete was accompanied by low D_s values. Another study reported a similar negative relationship between the chloride permeability of concrete and the D_s. Since the D_s reflects the complexity and irregularity of the pores, and the pore parameters strongly affect the permeability of concrete, it can be reasonably concluded that the D_s can be used to characterize the impermeability property of face slab concrete.

In addition, the differences in the degree of permeability caused by the fly ash dosage could be interpreted in terms of the D_s. For instance, before 28 days, the addition of up to 50% fly ash coarsened the pores and reduced the D_s; thus, the K_r values were increased. In contrast, at 180 days, the addition of no more than 30% fly ash effectively

increased the proportion of fine pores ($V_{2.5–50\,nm}$) and inevitably increased the complexity and irregularity of pore structures, as well as the D_s values. Consequently, the K_r values were lowered.

4. Conclusions

The main results can be summarized as follows:

(1) The inclusion of 10–50% fly ash lowered the compressive strength of the face slab concrete by 6.2–8.5%, 12.6–16.4%, 16.8–25.6%, 24.9–36.2% and 33.2–47.2% before 28 days of hydration, respectively, whereas it contributed to the development of strength at 180 days.

(2) The incorporation of 10–50% fly ash raised the average water-seepage height (D_m) and the relative permeability coefficient (K_r) of the face slab concrete by about 14–81% and 30–226% at 28 days, respectively. At 180 days, the addition of less than 30% fly ash improved the 180-day impermeability of the face slab concrete. Beyond a dosage of 30%, the fly ash addition was detrimental to the concrete's impermeability.

(3) Before 28 days, with the fly ash dosage increased from 0% up to 50%, the pores in the concrete became larger and coarser, and the D_s values declined from 2.836–2.887 to 2.743–2.819. At 180 days, at the fly ash dosage of 30%, the fly ash clearly refined the pore structures of the face slab concretes and raised the D_s values from 2.911 to 2.947. As the fly ash dosage increased from 30% to 50%, the pore refinement effect weakened, and the 180-day D_s values were lowered from 2.947 to 2.885. The D_s values of the face slab concretes exhibited an obvious correlation with the porous structure.

(4) The permeability of the face slab concretes is closely correlated with the pore structures and D_s. The fly ash addition of no more than 30% effectively increased the fine pore proportions and raised the complexity and irregularity of pores, as well as increasing the D_s values at 180 days. Consequently, this lowered the K_r values.

(5) The optimal fly ash dosage, in terms of the long-term impermeability and pore refinement of face slab concretes, is around 30%, as such an optimal fly ash dosage does not appear to weaken the compressive strength. Nevertheless, face slab concrete containing a high dosage of fly ash must be cured for a relatively long period before it can withstand high water pressure.

Future perspective: The influences of fly ash on the microstructures, frost resistance and deformation properties of face slab concrete will be investigated using more varied techniques, including XRD, SEM/energy dispersive X–ray (EDX) and Fourier infrared spectrometry (FTIR). Additionally, other kinds of fractal dimensions with different physical values, such as the pore volume fractal dimension and the pore tortuosity fractal dimension, will be considered in order to evaluate the structures and properties of concrete in our future work.

Author Contributions: Conceptualization, writing—original draft, writing—review and editing, investigation, formal analysis, supervision, project administration and funding acquisition, L.W.; investigation and formal analysis, S.Z., Y.S., Y.H., F.Z., T.H. and S.T. All authors have read and agreed to the published version of the manuscript.

Funding: The authors express their thanks to the National Natural Science Foundation of China (funding number: 51779019 and 52179122) and the Opening Funds of the Belt and Road Special Foundation of the State Key Laboratory of Hydrology—Water Resources and Hydraulic Engineering (funding number: 2020492311).

Institutional Review Board Statement: Not applicable.

Informed Consent Statement: Not applicable.

Data Availability Statement: The data that support the findings of this study are available from the corresponding author upon reasonable request.

Acknowledgments: The authors would like to thank all the anonymous referees for their constructive comments and suggestions.

Conflicts of Interest: The authors declare no conflict of interests.

References

1. Zheng, Y.; Shan, K.; Xu, Y. Numerical simulation of mechanical characteristics of concrete face rockfill dam under complicated geological conditions. *Arab. J. Geosci.* **2019**, *12*, 674. [CrossRef]
2. Cen, W.J.; Wen, L.S.; Zhang, Z.Q.; Xiong, K. Numerical simulation of seismic damage and cracking of concrete slabs of high concrete face rockfill dams. *Water Sci. Eng.* **2016**, *9*, 205–211. [CrossRef]
3. Salajegheh, P.; Habibagahi, G.; Sahraeian, S.M.S. Utilizing fiber reinforced concrete as the concrete face of rockfill dams. *Ksec. J. Civ. Eng.* **2019**, *23*, 1077–1086. [CrossRef]
4. Qu, Y.Q.; Zou, D.G.; Kong, X.J.; Liu, J.M.; Zhang, Y.; Yu, X. Seismic damage performance of the steel fiber reinforced face slab in the concrete-faced rockfill dam. *Soil Dyn. Earthq. Eng.* **2019**, *119*, 320–330. [CrossRef]
5. Ma, H.Q.; Chi, F.D. Technical progress on researches for the safety of high concrete-faced rockfill dams. *Engineering* **2016**, *2*, 332–339. [CrossRef]
6. Qin, Z.P.; Lai, Y.M.; Tian, Y.; Yu, F. Frost-heaving mechanical model for concrete face slabs of earthen dams in cold regions. *Cold Reg. Sci. Technol.* **2019**, *161*, 91–98. [CrossRef]
7. Huang, W.F.; Li, Z.J.; Han, H.W.; Jia, Q. Limit resistive forces from ice frozen to concrete-revetment interface of an inclined dam wall. *Cold Reg. Sci. Technol.* **2017**, *141*, 181–187. [CrossRef]
8. Bouchenafa, O.; Hamzaoui, R.; Bennabi, A.; Colin, J. PCA effect on structure of fly ashes and slag obtained by mechanosynthesis. Applications: Mechanical performance of substituted paste CEMI + 50% slag/or fly ashes. *Constr. Build. Mater.* **2019**, *203*, 120–133. [CrossRef]
9. Yang, B.B.; Liu, J.W.; Zhao, X.M.; Zheng, S. Evaporation and cracked soda soil improved by fly ash from recycled materials. *Land Degrad. Dev.* **2021**, *32*, 2823–2832. [CrossRef]
10. Yang, B.B.; Li, D.D.; Yuan, S.C.; Jin, L.C. Role of biochar from corn straw in influencing crack propagation and evaporation in sodic soils. *Catena* **2021**, *204*, 105457. [CrossRef]
11. Zhang, P.; Kang, L.; Zheng, Y.; Zhang, T.; Zhang, B. Influence of SiO2 /Na2O molar ratio on mechanical properties and durability of metakaolin-fly ash blend alkali-activated sustainable mortar incorporating manufactured sand. *J. Mater. Res. Technol.* **2022**, *18*, 3553–3563. [CrossRef]
12. Akid, A.S.M.; Hossain, S.; Munshi, M.I.U.; Elahi, M.M.A.; Sobuz, M.H.R.; Tam, V.W.Y.; Islam, M.S. Assessing the influence of fly ash and polypropylene fiber on fresh, mechanical and durability properties of concrete. *J. King Saud Univ.-Eng. Sci.* 2021, *accepted, in press*. [CrossRef]
13. Bogă, A.R.; Topçu, I.B. Influence of fly ash on corrosion resistance and chloride ion permeability of concrete. *Constr. Build. Mater.* **2012**, *31*, 258–264. [CrossRef]
14. Liu, J.; Ou, G.; Qiu, Q.; Chen, X.; Hong, J.; Xing, F. Chloride transport and microstructure of concrete with/without fly ash under atmospheric chloride condition. *Constr. Build. Mater.* **2017**, *146*, 493–501. [CrossRef]
15. Kizilkanat, A.B.; Oktay, D.; Kabay, N.; Tufekci, M.M. Comparative experimental study of mortars incorporating pumice powder or fly ash. *J. Mater. Civ. Eng.* **2016**, *28*, 04015119. [CrossRef]
16. Yu, Y.; Yu, J.; Ge, Y. Water and chloride permeability research on ordinary cement mortar and concrete with compound admixture and fly ash. *Constr. Build. Mater.* **2016**, *127*, 556–564. [CrossRef]
17. Yu, Z.; Ni, C.; Tang, M.; She, X. Relationship between water permeability and pore structure of Portland cement paste blended with fly ash. *Constr. Build. Mater.* **2018**, *175*, 458–466. [CrossRef]
18. Zhang, X.; Zhang, P.; Wang, T.; Zheng, Y.; Qiu, L.; Sun, S. Compressive strength and anti-chloride ion penetration assessment of geopolymer mortar merging PVA fiber and nano-SiO2 using RBF–BP composite neural network. *Nanotechnol. Rev.* **2022**, *11*, 1181–1192. [CrossRef]
19. Wang, J.; Guo, Z.; Yuan, Q.; Zhang, P.; Fang, H. Effects of ages on the ITZ microstructure of crumb rubber concrete. *Constr. Build. Mater.* **2020**, *254*, 119329. [CrossRef]
20. Zheng, J.J.; Wong, H.S.; Buenfeld, N.R. Assessing the influence of ITZ on the steady-state chloride diffusivity of concrete using a numerical model. *Cem. Concr. Res.* **2009**, *39*, 805–813. [CrossRef]
21. Metha, P.K.; Monterio, P.J.M. *Concrete: Structure, Properties, and Materials*, 4th ed.; McGraw-Hill: New York City, NY, USA, 2013.
22. Wu, K.; Shi, H.S.; Xu, L.L.; Ye, G.; De Schutter, G. Microstructural characterization of ITZ in blended cement concretes and its relation to transport properties. *Cem. Concr. Res.* **2016**, *79*, 243–256. [CrossRef]
23. Zeng, Q.; Luo, M.Y.; Pang, X.Y.; Li, L.; Li, K.F. Surface fractal dimension: An indicator to characterize the microstructure of cement-based porous materials. *Appl. Surf. Sci.* **2013**, *282*, 302–307. [CrossRef]
24. Yu, P.; Duan, Y.H.; Chen, E.; Tang, S.W.; Wang, X.R. Microstructure-based fractal models for heat and mass transport properties of cement paste. *Int. J. Heat Mass Transf.* **2018**, *126*, 432–447. [CrossRef]
25. Zarnaghi, V.N.; Fouroghi-Asl, A.; Nourani, V.; Ma, H.Y. On the pore structures of lightweight self-compacting concrete containing silica fume. *Constr. Build. Mater.* **2018**, *193*, 557–564. [CrossRef]
26. Yang, B.; Liu, Y. Application of fractals to evaluate fractures of rock due to mining. *Fractal Fract.* **2022**, *6*, 96. [CrossRef]
27. Luan, C.; Wang, J.; Gao, J.; Wang, J.; Du, P.; Zhou, Z.; Huang, Y.; Du, S. Changes in fractal dimension and durability of ultra-high performance concrete (UHPC) with silica fume content. *Arch. Civ. Mech. Eng.* **2022**, *22*, 123. [CrossRef]
28. Chen, J.; Zhao, H.; Zhao, M.; Peng, W.; Hou, J. Prediction of permeability for fully weathered granite amended with fly ash by fractal dimensions. *J. Sustain. Cem. Mater.* **2022**, *2*, 2042750. [CrossRef]

29. *GB 175-2007*; Common Portland Cement, China. China Standard Press: Beijing, China, 2007.
30. *DL/T 5016-2011*; Design Code for Concrete Faced Rockfill Dams, China. China Electric Power Press: Beijing, China, 2011.
31. *DL/T 5150-2017*; Test Code for Hydraulic Concrete, China. China Electric Power Press: Beijing, China, 2017.
32. Yuan, B.; Li, Z.; Zhao, Z.; Ni, H.; Su, Z.; Li, Z. Experimental study of displacement field of layered soils surrounding laterally loaded pile based on transparent soil. *J. Soils Sediments* **2021**, *21*, 3072–3083. [CrossRef]
33. Zhang, Y.; Zhang, X.; Cai, X.; Gao, L.; Li, Q.; Kong, X. A further understanding on the strength development of cement pastes in the presence of triisopropanolamine used in CRTS III slab track. *Constr. Build. Mater.* **2022**, *315*, 125743. [CrossRef]
34. Yuan, B.; Li, Z.; Chen, Y.; Hong, N.; Zhao, Z.; Chen, W.; Zhao, J. Mechanical and microstructural properties of recycling granite residual soil reinforced with glass fiber and liquid-modified polyvinyl alcohol polymer. *Chemosphere* **2021**, *268*, 131652. [CrossRef]
35. Yuan, B.; Sun, M.; Wang, Y.; Zhai, L.; Luo, Q.; Zhang, X. Full 3D displacement measuring system for 3D displacement field of soil around a laterally loaded pile in transparent soil. *ASCE Int. J. Geomech.* **2019**, *19*, 04019028. [CrossRef]
36. Jin, S.S.; Zhang, J.X.; Huang, B.S. Fractal analysis of effect of air void on freeze–thaw resistance of concrete. *Constr. Build. Mater.* **2013**, *47*, 126–130. [CrossRef]
37. Zhang, B.Q.; Li, S.F. Determination of the surface fractal dimension for porous media by mercury porosimetry. *Ind. Eng. Chem. Res.* **1995**, *34*, 1383–1386. [CrossRef]
38. Zhang, B.Q.; Liu, W.; Liu, X. Scale-dependent nature of the surface fractal dimension for bi- and multi-disperse porous solids by mercury porosimetry. *Appl. Surf. Sci.* **2006**, *253*, 1349–1355. [CrossRef]
39. Yin, B.; Kang, T.; Kang, J.; Chen, Y.; Wu, L.; Du, M. Investigation of the hydration kinetics and microstructure formation mechanism of fresh fly ash cemented filling materials based on hydration heat and volume resistivity characteristics. *Appl. Clay Sci.* **2018**, *166*, 146–158. [CrossRef]
40. Termkhajornkit, P.; Nawa, T.; Kurumisawa, K. Effect of water curing conditions on the hydration degree and compressive strengths of fly ash–cement paste. *Cem. Concr. Compos.* **2006**, *28*, 781–789. [CrossRef]
41. Hu, X.; Shi, Z.G.; Shi, C.J.; Wu, Z.M.; Tong, B.H.; Ou, Z.H.; de Schutter, G. Drying shrinkage and cracking resistance of concrete made with ternary cementitious components. *Constr. Build. Mater.* **2017**, *149*, 406–415. [CrossRef]
42. Yoon, Y.S.; Won, J.P.; Woo, S.K. Enhanced durability performance of fly ash concrete for concrete-faced rockfill dam application. *Cem. Concr. Res.* **2002**, *32*, 23–30. [CrossRef]
43. Zhang, P.; Gao, Z.; Wang, J.; Guo, J.; Wang, T. Influencing factors analysis and optimized prediction model for rheology and flowability of nano-SiO2 and PVA fiber reinforced alkali-activated composites. *J. Clean. Prod.* **2022**, *366*, 132988. [CrossRef]
44. Termkhajornkit, P.; Nawa, T.; Nakai, M.; Saito, T. Effect of fly ash on autogenous shrinkage. *Cem. Concr. Res.* **2005**, *35*, 473–482. [CrossRef]
45. Oner, A.; Akyuz, S.; Yildiz, R. An experimental study on strength development of concrete containing fly ash and optimum usage of fly ash in concrete. *Cem. Concr. Res.* **2005**, *35*, 1165–1171. [CrossRef]
46. Poon, C.S.; Lam, L.; Wong, Y.L. A study on high strength concrete prepared with large volumes of low calcium fly ash. *Cem. Concr. Res.* **2000**, *30*, 447–455. [CrossRef]
47. Wang, L.; Yang, H.Q.; Zhou, S.H.; Chen, E.; Tang, S.W. Mechanical properties, long-term hydration heat, shinkage behavior and crack resistance of dam concrete designed with low heat Portland (LHP) cement and fly ash. *Constr. Build. Mater.* **2018**, *187*, 1073–1091. [CrossRef]
48. Wang, J.; Guo, Z.; Zhang, P.; Yuan, Q.; Guan, Q. Fracture properties of rubberized concrete under different temperature and humidity conditions based on digital image correlation technique. *J. Clean. Prod.* **2020**, *276*, 124106. [CrossRef]
49. Sakai, E.; Miyahara, S.; Ohsawa, S.; Lee, S.H.; Daimon, M. Hydration of fly ash cement. *Cem. Concr. Res.* **2005**, *35*, 1135–1140. [CrossRef]
50. Moghaddam, F.; Sirivivatnanon, V.; Vessalas, K. The effect of fly ash fineness on heat of hydration, microstructure, flow and compressive strength of blended cement pastes. *Case Stud. Constr. Mater.* **2019**, *10*, e00218. [CrossRef]
51. Mindess, S.; Young, J.F.; Darwin, D. *Concrete*; Prentice-Hall: Murray Hill: NJ, USA, 2003.
52. Zeng, Q.; Li, K.F.; Teddy, F.C.; Patrick, D.L. Surface fractal analysis of pore structure of high-volume fly-ash cement pastes. *Appl. Surf. Sci.* **2010**, *257*, 762–768. [CrossRef]
53. Lü, Q.; Qiu, Q.L.; Zheng, J.; Wang, J.Y.; Zeng, Q. Fractal dimension of concrete incorporating silica fume and its correlations to pore structure, strength and permeability. *Constr. Build. Mater.* **2019**, *228*, 116986. [CrossRef]